Available online at www.sciencedirect.com
ScienceDirect
Journal of Power Sources 164 (2007) 934–946
JOURNAL OF POWER SOURCES
www.elsevier.com/locate/jpowsour

Effects of cationic CTAB and anionic SDBS surfactants on the performance of Zn–MnO_2 alkaline batteries

Robab Khayat Ghavami *, Zahra Rafiei, S. Mojtaba Tabatabaei

R & D Center, Niru Battery MFG. Co., P.O. Box 19575-361, Tehran, Islamic Republic of Iran

Received 6 May 2006; received in revised form 18 October 2006; accepted 24 October 2006
Available online 4 December 2006

Abstract

Inhibiting properties of two kinds of surfactant, cationic cetyl trimethyl ammonium bromide (CTAB) and anionic sodium dodecyl benzene sulfonate (SDBS) with three different concentrations, in relation to zinc passivation have been explained in the primary Zn/MnO_2 alkaline batteries. Discharge performance of alkaline cell affected by utilization of surfactant in anodic gel. Therefore, electrochemical properties of anodic zinc have been investigated by cyclic voltammetry, X-ray diffraction, scanning electron microscopy (SEM) and ac impedance techniques. The results show that alkaline cell with 0.01 g l^{-1} of anionic SDBS surfactant decreased effectively the rate of zinc-passivation reaction. Also, it exhibited ZnO morphology with smaller grain size, causing longer service life gradually, step by step.

By contrast, 0.01 g l^{-1} of cationic CTAB surfactant remarkably increased the rate of charge transfer and mass transfer in the alkaline cell, on impedance data. Consequently, more volumetric energy density obtained in first discharge step due to more activated zinc surface area. Furthermore, scanning electron microscopy (SEM) has shown non-homogenous morphology with coarse ZnO growth. This was confirmed by X-ray diffractograms showing the highest intensity of ZnO peak. When the concentration of these surfactants (CTAB and SDBS) increased, more inhibiting properties were observed. This property was stronger in the cells with anionic SDBS surfactant. Our study is mainly focused on the understanding the mechanism of zinc passivation in the presence of the surfactants.

Keywords: Surfactants; Alkaline Zn/MnO_2 Battery; Zinc passivation; Crystal growth; Electrochemical capacity

1. Introduction

Since its introduction in the early 1960s, the Zn/MnO_2 alkaline battery has become the dominate battery system in portable battery market. Zinc has a wide variety of applications as a negative electrode material in Zn–Mn, Zn–Ag, Zn–Ni and Zn–air batteries. The zinc based batteries are noted for its low equilibrium potential, good reversibility, high specific energy, and volumetric energy density, low cost and low toxicity. Hence, advances in rechargeable zinc batteries have included the use of additives and modified charging methods to obtain a beneficial effect on considering problems of zinc electrode like dendritic growth, hydrogen evolution, shape change and high dissolution [1–6].

Huot and Malservisi [7] have studied the high rate capability of zinc electrodes in a primary alkaline Zn–MnO_2 cell in terms of zinc anode formulation, including zinc alloy composition and the particles size-distribution. It was concluded that the utilization of metallic zinc was very low under the high rate discharge condition. For an LR6 cell (AA size) containing 3.6 g zinc powder, the actual zinc material utilization is only 25% under 1 A continuous discharge experiment. Furthermore, one of the most successful approaches to study battery electrodes is applying suitable surfactants to overcome these problems, because the mechanism of zinc dissolution changes with the types of additives such as organic [8,9] or inorganic compounds [10] on composition of electrolyte solution. In practice, it is well known that the introduction of small amounts of some surfactants affects on the growth of zinc moss and dendrites through the control of the electrode passivation [11,12]. Also Yang et al. improved discharge capacity and suppressed surface passivation of zinc anode in dilute alkaline solution using surfactant additives [13].

* Corresponding author. Tel.: +98 21 22547034; fax: +98 21 22582421.
E-mail address: star_khayat@yahoo.com (R.K. Ghavami).

0378-7753/$ – see front matter © 2006 Elsevier B.V. All rights reserved.
doi:10.1016/j.jpowsour.2006.10.084

Surfactants are organic compounds consisting of two parts: a water-loving (hydrophilic) portion and a water-hating (hydrophobic) portion. Today such substances are used for these purposes: improving the wetting ability, emulsifying, increasing the inhibiting properties of electrodeposition process, etc. [14].

The specific activity of the surfactants is generally understood in terms of adsorption at the anode surface during electrochemical reaction and depends on the concentration of the surfactant molecules. When the concentration approaches the critical micelle concentration (cmc), the formation of bilayers or multilayer at the electrode interface occurs [15]. The adsorption of surfactant aggregates on the electrodes can have large effects not only on the kinetics of the electron transfer, which include blocking of active sites and consequently on the high rate discharge capability. But also it affects on electrostatic interaction between electroactive species and adsorbed surfactants [16]. According to these effects, it is possible to modify the growth mode of the crystals and tailor the morphology and structure of the product such as the modification of ZnO growth by application of suitable amount of specific surfactants. So the modified electrode is expected to supply superior mass transfer properties through regular mesoporous networks as a result of modified growth on the surface of adsorbed organic surfactant layers. Consequently, such modifications affect the morphology, crystallinity, mechanical properties and electrochemical activity of materials [17]. Therefore, surfactants and non-soluble oily materials can form micelles with diverse shapes [18], which can control the kinetics of electron transfer and the electrode morphology. This control can lead to high porosity in electrode and maximum energy density in batteries due to very interesting and unique properties of these materials.

In the present study, the effects of two surfactants, cationic cetyl trimethyl ammonium bromide (CTAB) and anionic sodium dodecyl benzene solfonate (SDBS), at three different concentrations have been investigated. Also it have been tried systematically to understand the basic mechanism of the zinc dissolution in Zn–MnO_2 batteries because the reaction mechanism of zinc dissolution and its dependence upon the presence of surfactants additives is not well understood yet and it could be special interest. The logical aims of this study is investigation zinc dissolution–passivation processes in the presence of surfactant in discharge process and optimize anode composition of Zn–MnO_2 alkaline batteries. In such a way, the electrode will have the minimum shape change, the longest service life and superior mass transfer property by studying results of discharge experiment, X-ray diffraction, scanning electron microscopy (SEM) and ac impedance techniques.

2. Experimental

The AA-size Zn/MnO_2 cells with similar cathodic rings, separators and steel cans (taken from commercial AA-size alkaline Zn/MnO_2 cells) were used to study of anode gel whose composition was changed by using different amounts of two kinds of surfactant. The anodes were gelled by mixing 30% electrolyte (9 M KOH + surfactant), 68% commercial zinc, 1% zinc oxide, 1% C.M.C. (carboxylic methyl cellulose).

Table 1
The name of cells was fabricated with various amounts of two kinds of surfactant which added in anodic portion

Additives	Amount of additives ($g\,l^{-1}$)	Name of batteries
CTAB	0.01	0.01 CT cell
CTAB	0.05	0.05 CT cell
CTAB	0.1	0.1 CT cell
SDBS	0.01	0.01 SD cell
SDBS	0.05	0.05 SD cell
SDBS	0.1	0.1 SD cell

Different amounts (0.01, 0.05 and 0.1 g) of surfactants, cationic (CTAB) and anionic (SDBS) were added to a liter of electrolyte solutions. The cells, which were fabricated with these different anode gels, are called with different names and listed in Table 1.

Cyclic voltammograms for zinc electrode were obtained in 9 M KOH with different amount of given both surfactants. Polarization experiments were performed by means of Autolab PGSTAT 30 in the range −1800 to −0.5 at a constant scan rate of $10\,mV\,s^{-1}$.

ac impedance measurements were carried out by using an electrochemical impedance analyzer (Potentiostat/Galvanostat, SI1260, Solarton Inst., UK) and Zplot & Zview software.

The ac excitation signal was 5 mV at open circuit conditions of the cell and the frequencies range was between 100 kHz and 10 mHz. All experiments were carried out in an air-conditioned room at 20 °C.

All the fresh cells were discharged under 500 mA constant current. The discharge of each cell was stopped at 0.1 V and cells were put on rest for 60 min. After discharge, the cell was allowed to equilibrate at OCV conditions. The value of SOC was taken as 0 when the cell voltage reached 0.1 V during discharge. The ac impedance measurements were carried out at SOC100 and SOC0.

The morphology of the ZnO grown films was investigated in the discharged cells by scanning electron microscopy (Philips XL30) and XRD diffraction. Powder X-ray diffraction (XRD) patterns were recorded by using a Philips Xpert diffractometer and Cu Kα radiation (λ = 0.15418 nm).

3. Results and discussions

3.1. Reactions of the alkaline Zn–MnO_2 cell

A Zn–MnO_2 cell consists of a positive electrode mainly made of EMD (electrolytic manganese dioxide) and a negative electrode almost made of Zn in 9 M KOH solution as electrolyte. The electrode reactions are reversible in nature, even though the cycle–life of the primary alkaline Zn–MnO_2 cell is generally reported to be rather limited. During discharge of an alkaline Zn–MnO_2 cell, the following reactions take place. At the cathode, the reduction of MnO_2 occurs in two steps:

$$MnO_2 + H_2O + e^- \Leftrightarrow MnOOH + OH^- \quad (1)$$

$$MnOOH + H_2O + e^- \Leftrightarrow Mn(OH)_2 + OH^- \quad (2)$$

The first reaction represents a homogenous reduction of MnO_2 to MnOOH, and the second reaction indicates reduction of MnOOH to $Mn(OH)_2$ in a heterogeneous mechanism involving Mn^{3+} ions in the electrolyte. The second reaction depends on KOH concentration and current density [19].

The electrochemical reaction of the zinc electrode in a negative electrode proceeds via dissolution–precipitation reaction [20]. The reaction mechanism involves the formation of supersaturated zincate solution through the following electron transfer reaction:

$$Zn + 4OH^- \Leftrightarrow Zn(OH)_4^{2-} + 2e^- \quad (3)$$

From $Zn(OH)_4^{2-}$, the formation of porous ZnO on the electrode surface takes place by the following chemical reaction:

$$Zn(OH)_4^{2-} \Leftrightarrow ZnO + 2OH^- + H_2O \quad (4)$$

The high solubility of zincate in KOH solution leads into non-uniform deposition of ZnO, shape change, formation of dendrites and the development of inter-electrode short-circuits [21].

The capacity of alkaline cell is limited by the Zn anode because the potential of the Zn anode shows a reduction at the end of discharge of the alkaline cell, while the potential of the MnO_2 cathode remains constant during discharge cell. Also, the magnitude of the impedance of the MnO_2 cathode is several times smaller than the alkaline cell or the Zn anode. This observation suggests that the cell impedance is dominated by the anode [22,23].

3.2. Electrochemical performance

All the fresh cells (listed in Table 1) were discharged to 0.1 V under 500 mA constant current at the room temperature. The discharge curves of CT and SD cells are given in Fig. 1a and b, respectively. Also, each Figure includes the discharge curve of without surfactant. Fig. 1a compares two types of curve for discharged cells: flat curves; including 0.01 CT and 0.05 CT cells, with longer discharge time, and sloping curves; containing without surfactant cell and 0.1 CT cell, with shorter discharge time. In 0.01 CT and 0.05 CT cells, the voltage is started above 1.5 V and decreased rapidly. It can be related to the non-homogeneous phase discharge of zinc. Moreover, the discharge time of CT cells were longer than without surfactant cell. Also, Fig. 1a shows the improvement of electrochemical capacity through increasing order: without surfactant < 0.1 CT < 0.05 CT < 0.01 CT.

Fig. 1b represents discharge curves of without surfactant cell and SD cells. It is clear that the cell with the flat discharge profile gives the longer service life because 0.01 SD cell with the flat discharge curve represents the longest discharge time. Also,

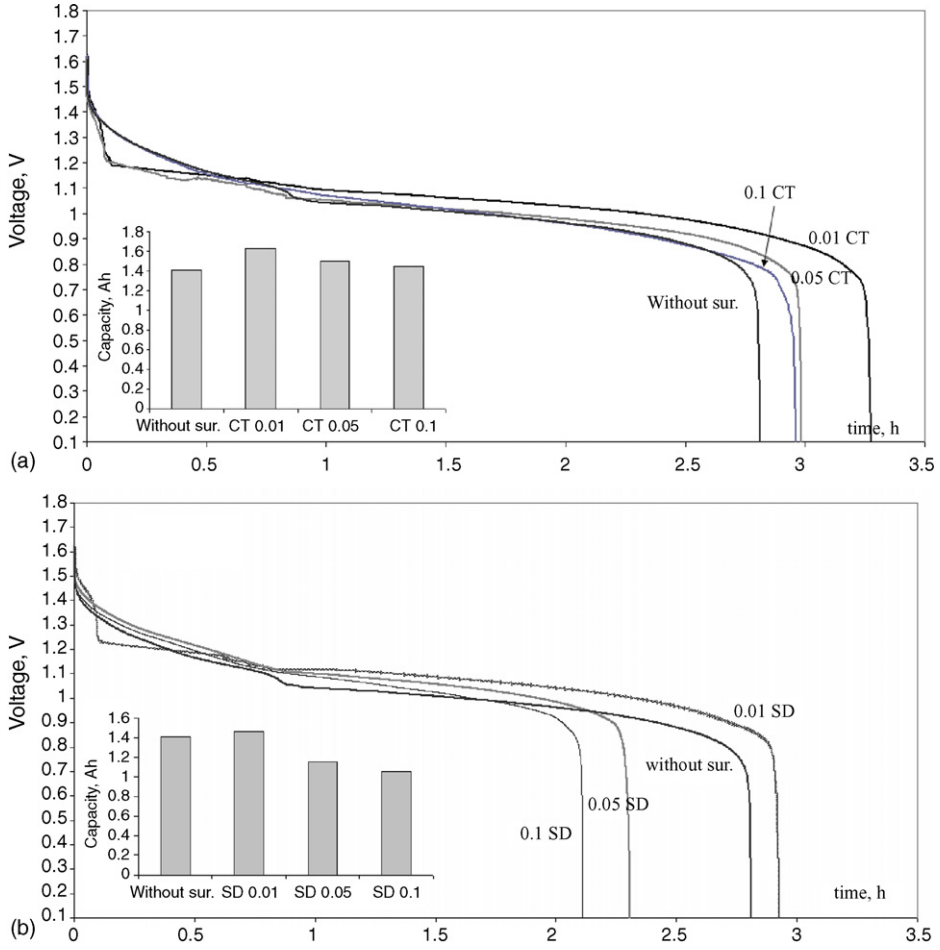

Fig. 1. Discharge curves and electrochemical capacity: (a) without surfactant and CT cells and (b) without surfactant and SD cells.

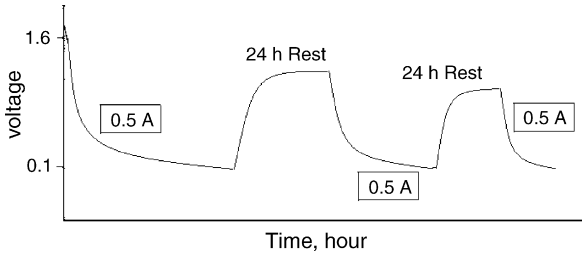

Fig. 2. The profile used for testing all cells.

Fig. 1b shows the reduction of electrochemical capacity with the following order: 0.1 SD < 0.05 SD < without surfactant < 0.01 SD.

The comparison of both figures (Fig. 1a and b) shows that CT cells with the flat discharge curves indicate longer service life than SD cells. Since, CT cells could operate to wider voltage range than SD cells.

The cells were then subjected of the profile shown in Fig. 2. The profile is composed of several constant current (0.5 A) steps and resting steps (24 h). In each step, all alkaline cells were discharged under 500 mA constant current. The discharge of each cell was stopped at 0.1 V and cells were put on rest for 24 h.

After the first resting step, the results show that, 0.01 CT, 0.05 CT and without surfactant cells were not discharged again while 0.1 CT cell was discharged for a short time. But SD cells were discharged more than three times according to Fig. 3a. Also Fig. 3b shows the corresponding total electrochemical capacity of these cells.

In Fig. 3a, the electrochemical capacity of SD cells decreased after the each discharge step. During the second and third discharge steps, 0.01 SD cell caused a higher capacity loss per cycle, compared to 0.1 and 0.05 SD cells. Apparently, the high concentration of anionic SDBS surfactant has the beneficial effect of increasing gradually service life during the discharge steps. The high electrochemical capacity of 0.01 SD cell can arise from more zinc utilization at the first discharge step.

It is to say, if the cells are dischargeable for several times, the service life of the cell will be longer. According to the above, the service life of SD cells especially 0.05 SD and 0.1 SD with sloping discharge curves could be extended and exceeded in comparison with CT cells and without surfactant cell, which have the flat discharge profile. Therefore, SD cells exhibit higher service life. Inhibiting effect of anionic SDBS surfactant especially in the high concentration caused the high energy storing. By contrast, cationic CTAB surfactant increases the rate of passivation reaction because these cells released all the electrochemical energy just in the once discharge step.

A comparison of the discharge performance for the fabricated AA-size alkaline Zn/MnO_2 cells showed that: The percentage of capacity retention depends on the kind and concentration of surfactants, since the 0.1 and 0.05 SD cells with sloping discharge curve cause the high capacity retention during discharge process.

In addition, in the presence of anionic SDBS surfactant, the zinc anode reaction was restricted due to inhibiting effect. Probably, the inhibiting properties of anionic SDBS surfactant makes the anode reaction more reversible, while cationic CTAB surfactant leads to further discharge of zinc even more than in the absence of surfactant molecules. Thus, more zincate produce in CT cells, especially 0.01 CT. Also, when the concentration of both surfactants increases the discharge performance of these cells decreases, showing more inhibiting effect on dissolution reaction and zinc passivation, especially in the presence of anionic SDBS surfactant.

3.3. Cyclic voltammetry

The working electrode was prepared from high purity zinc (anal. 99.9%, Merck product) and made into a cylindrical rod with a diameter of 1 cm^2. The rod was embedded in a Teflon gasket and fitted with a suitable electrical connection. Prior to each experiment, the zinc electrode was first polished with emery papers (1000, 2000, 3000 and 4000), until a mirror surface was obtained. A platinum sheet was used as a counter electrode.

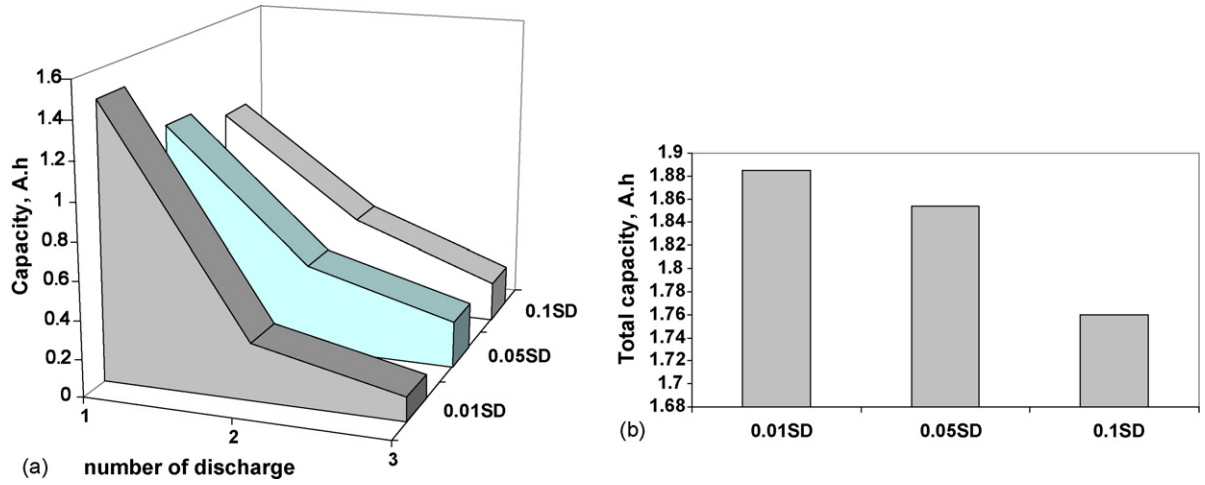

Fig. 3. Discharge capacity of SD cells at first, second and third discharge (a), and its total electrochemical capacity obtained of SD cells (b).

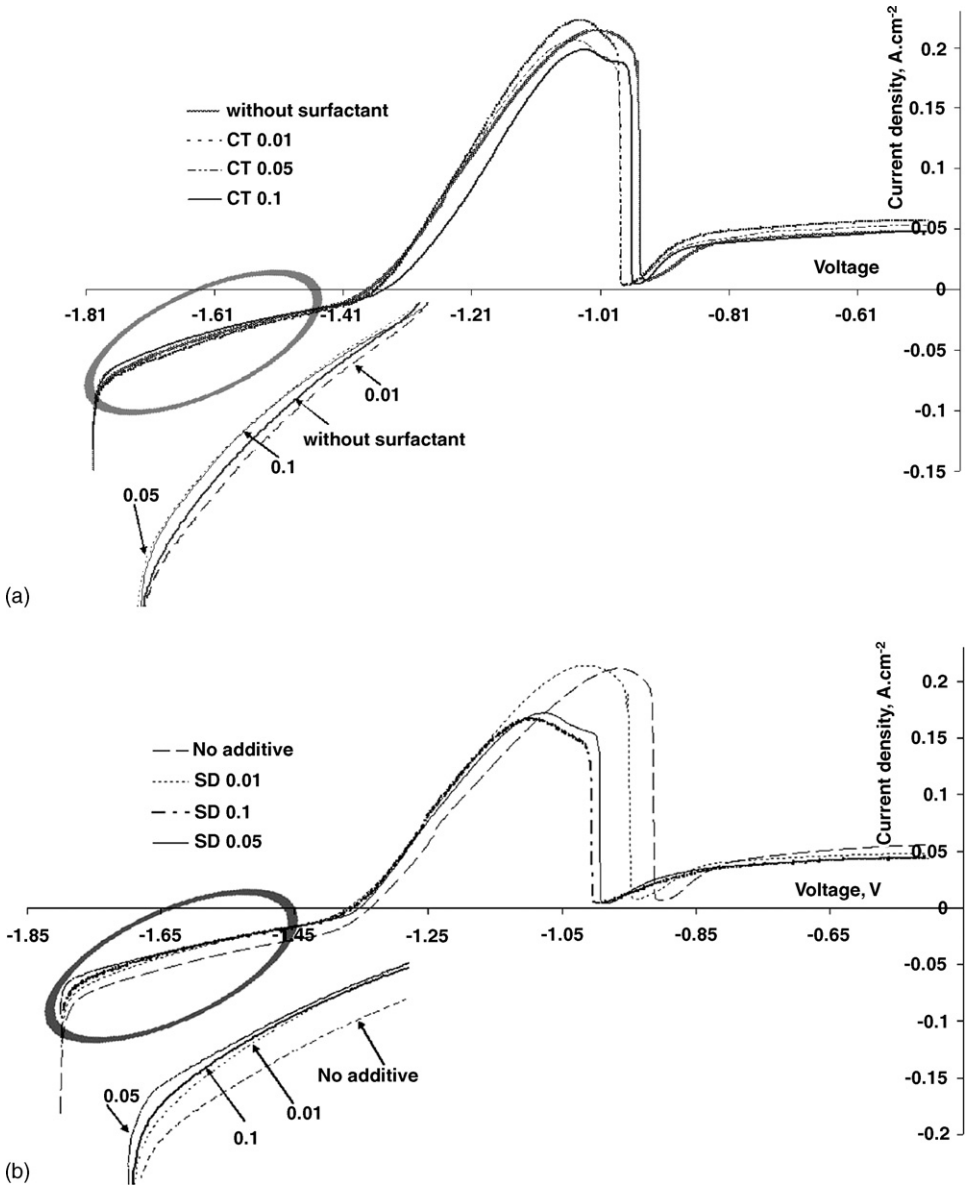

Fig. 4. Cyclic voltammograms for zinc dissolution in 9 M KOH. (a) CTAB surfactant and (b) SDBS surfactant.

An Hg/HgO with a Luggin capillary was used as a reference electrode.

Fig. 4a and b shows the electrochemical spectrum for a solid zinc electrode in 9 M KOH solution. The electrolyte composition was changed by various amount of surfactant. Fig. 4a corresponds to utilization of cationic CTAB surfactant and Fig. 4b represents anionic SDBS surfactant spectrums, at different concentration. On starting from −1800 mV, anodic peaks appear in the potential range −900 to −1100 mV at 10 mV s^{-1} scan rate.

The cathodic current density, for hydrogen evolution in the presence of anionic SDBS surfactant, were lower than the measured current densities in an alkaline medium without surfactant and cationic CTAB surfactant, as shown in Fig. 4a and b. It is obvious that the increase of over potential is correlated to the decrease of the rate of hydrogen evolution. The hydrogen overpotential rises to some degrees in the presence of anionic SDBS surfactant. Thus, the addition of SDBS surfactant can make the rate of hydrogen evolution slow. Also, higher overpotential on the zinc surface obtained for hydrogen evolution, when concentration of SDBS surfactant increased (Fig. 4a).

By contrast, adding of 0.01 g l^{-1} cationic CTAB surfactant increased the rate of hydrogen evolution, compared to alkaline medium without surfactant. When the concentration of CTAB surfactant increased, the hydrogen evolution decreased, as shown in Fig. 4b. It seems that the high concentration of CTAB surfactant (0.05, 0.1 g l^{-1}) impede hydrogen evolution. In addition, many studies have confirmed that this overpotential can be raised by the presence of certain surfactant [11,24].

Moreover, the anodic peak is attributed to the zinc dissolution that forms a transiently soluble Zn^{2+} species [25]. Subsequent hindrance to zinc oxidation results through the formation of a film depends on $Zn(OH)_2$/ZnO. The formation of this film depends on the extent to which $Zn(OH)_2$ dissolves in KOH to

Table 2
Measured anodic charge for Zn electrode during potentiodynamic cycle

Content of 9 M KOH	Without	0.01 CT	0.05 CT	0.1 CT	0.01 SD	0.05 SD	0.1 SD
Charge (C)	13.03	14	12.9	12	12.5	10.5	10

form zincate. Also, the zinc oxidation reaction mainly involves a diffusion controlled process [26].

During anodic cycle, the charge electrodes were measured. The charge values for all experiments are presented in Table 2. The measured charge of zinc electrode in the absence of surfactant was more than anionic SDBS surfactant solution. While it was lower than cationic CTAB surfactant solution.

When the concentrations of the both CTAB and SDBS surfactant (0.05, 0.1 g l^{-1}) increased in alkali media, the anodic charges decreased. Thus, the charge under the peaks increases with the decrease of surfactant concentration. Consequently, the high concentration of SDBS surfactant can decrease the rate of zinc passivation in 9 M KOH solution. So, Zn^{2+} ions are formed difficultly when the concentration of anionic SDBS surfactant increases.

In the presence of cationic CTAB surfactant, the charge under the anodic peaks was greater than the others. Also the large increase of the charge electrode is observed in the presence of 0.01 g l^{-1} cationic CTAB surfactant, which can be arisen from high surface area, causing high dissolution-rate (as observed in Fig. 4a).

By contrast, in the presence of 0.1 g l^{-1} anionic SDBS surfactant the solubility of zincate is restricted via the reduction of the anodic peak surface area. Thus, less charge value obtained, showing inhibiting properties. The results of performed experiments point out a various passivation effects depending on the kind and quantity of surfactants.

3.4. SEM

The electrochemical studies have shown that the addition of small amounts of surfactant modify the ZnO formation. In order to determine whether these changes were reflected in the zinc morphology and composition, SEMs (scanning electron microscopy) studies were done. The morphology of ZnO crystals was established with SEM at the end of the first discharge step. The discharged anode gel of without surfactant cell, SD and CT cells were used to determine SEMs as shown in Figs. 5–7. The data show that the surface morphology and the crystal shape and size are remarkably affected by the presence and nature of surfactants.

Before discharging, in the absence of surfactant molecules, the morphology displays the amorphous zinc, composed of oval-shaped, cylindrical, non-porous particles (Fig. 5a). The morphology of applied commercial zinc was similar in all cells. The effect of the surfactants is reported, on zinc morphology after discharge as follows.

In the absence of surfactant molecules, the coarse growth of ZnO was observed on zinc surface (Fig. 5b). In 0.01 CT cell (Fig. 6a), two different shapes were seen in the form of needle and granular. In this case heterogeneous growth of crystals in the form of large needle-like was observed on zinc surface, constituted by cauliflower type agglomerates. This morphology indicates increasing of competition between nucleation and crystal growth due to more crystal growth.

In 0.05 CT cell (Fig. 6b), the crystals shape was well-distributed. They had uniform tubular and rod growth. More ZnO crystal growth was observed in 0.01 CT and 0.05 CT cells. Thus, surfactants have a strong influence on the ZnO crystal growth. The regular ZnO crystal with needle growth existed in 0.1 CT cell (Fig. 6c), but the grain size was relatively smaller. It seems that the rate of crystal growth is restricted at high concentration of surfactant.

The observed ZnO crystals in the presence of 0.05 anionic SDBS surfactant were granular in smaller size (Fig. 7b). Less needle growth was formed in 0.1 SD cell (Fig. 7c). The needle crystals in 0.1 SD cell were smaller than 0.01 SD cell (Fig. 7a and c). In comparison with CT cells, the grain size was smaller and

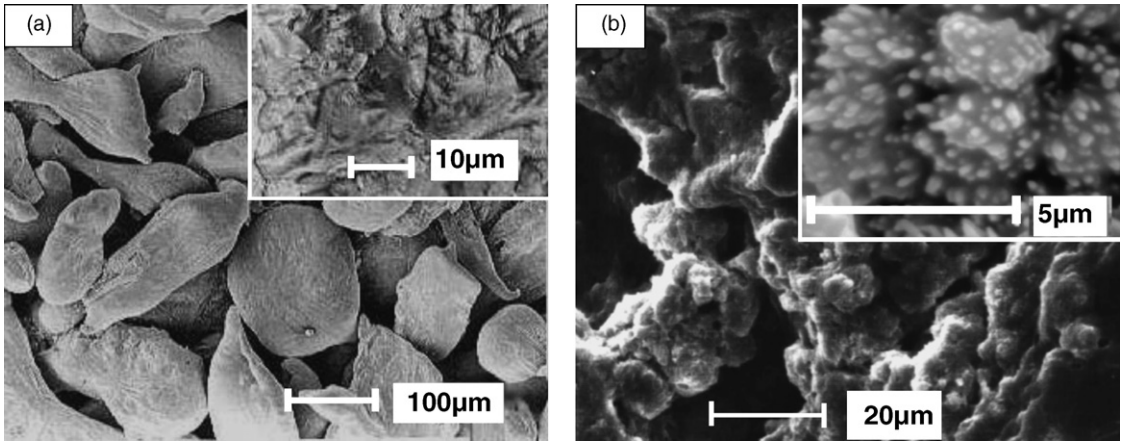

Fig. 5. Electron micrographs of the anode gel in the absence of surfactant molecules. (a) Before discharge and (b) after discharge.

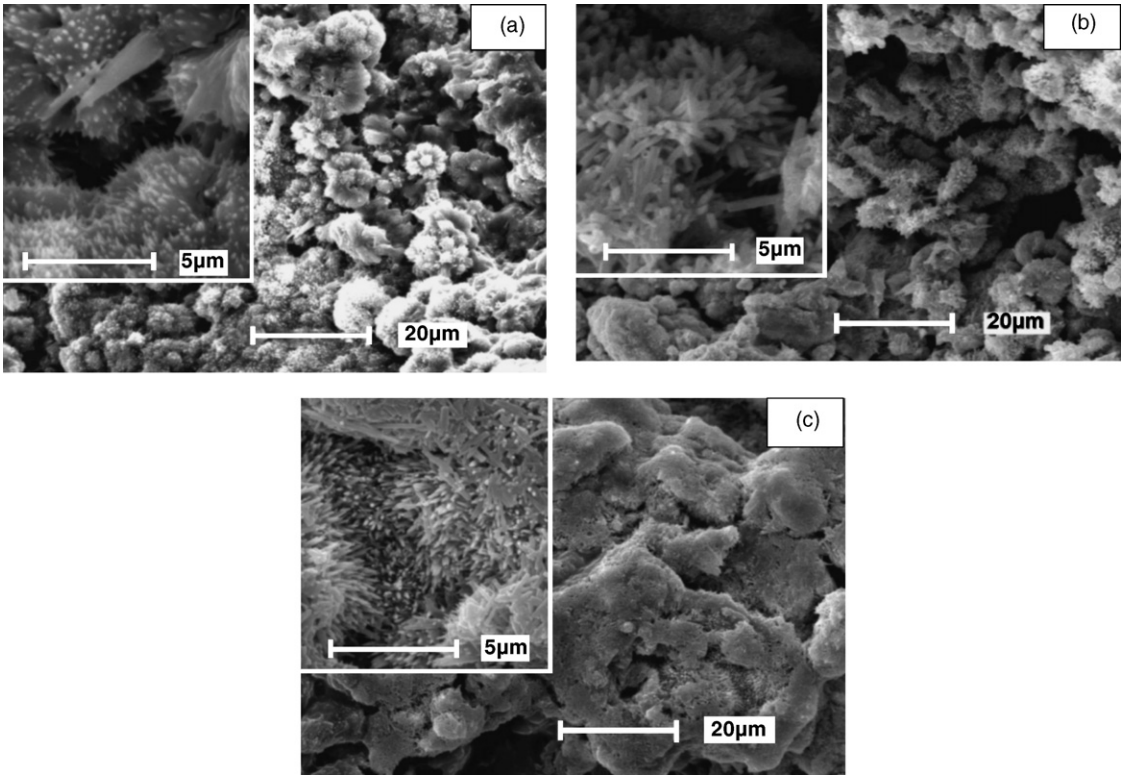

Fig. 6. Electron micrographs of the discharged anode gel in the presence of cationic CTAB surfactant. (a) 0.01 CT, (b) 0.05 CT and (c) 0.1 CT cells.

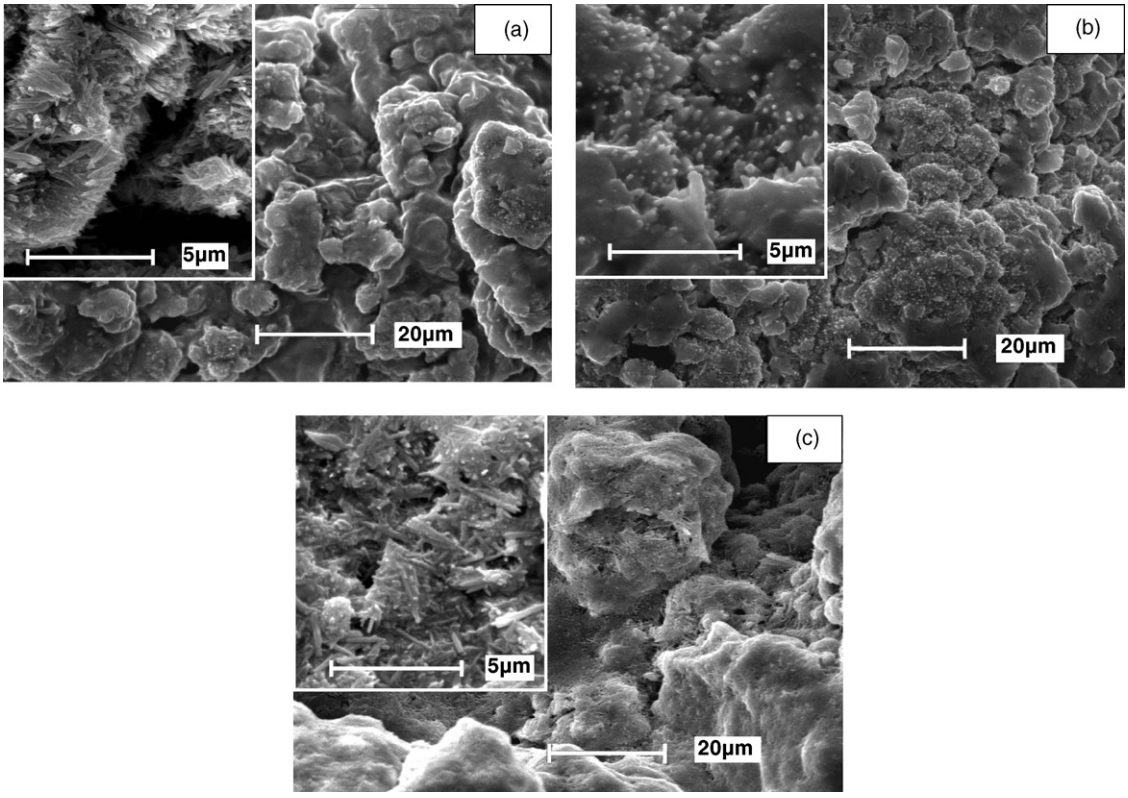

Fig. 7. Electron micrographs of the discharged anode gel in the presence of anionic SDBS surfactant. (a) 0.01 SD, (b) 0.05 SD and (c) 0.1 SD cells.

the crystal growth was more restricted to zinc surface. Therefore, the morphology change can be associated to a strong blocking effect of the anionic surfactant on zinc surface especially at the high concentration of surfactant.

3.5. X-ray diffraction

Fig. 6 displays the diffractograms of the obtained hexagonal ZnO crystal in all cells. It is clear that the presence of the surfactant in the anode gels, affects the crystallographic orientation and crystallinity.

In 0.01 CT and 0.05 CT cells, only diffraction peaks of ZnO were observed (Fig. 6a). While in the other cells (0.1 CT, 0.05 SD and 0.01 SD cells and without surfactant cell), the zinc and zinc oxide diffraction peaks were appeared, too. The position of appeared zinc texture lines is determined only on the without surfactant diffractogram (Fig. 8a). The most intensity of zinc diffraction line (1 0 1) is shown on the all diffractograms, except for 0.01 and 0.05 CT cells.

For the obtained ZnO from all cells (Fig. 8a–c), the lines with the most intensity diffraction are (1 0 1) and (1 0 3), respectively. In addition, a marked decrease on the (1 0 3) and (1 0 1) ZnO diffraction lines are found with the change of the surfactant kinds from cationic CTAB to anionic SDBS surfactant. Thus, the ZnO peak intensity strongly has affected by the kinds and concentration of surfactant (Fig. 8a and b).

According to Li and Szpunar [27], the development of different textures is possible during the growth of metal coating. This is a consequence of surface energy differences, which is responsible for the selective growth of the grain that has the lowest surface free energy. This process can take place in battery system because the conversion of zinc to zinc ions is an electrochemical reaction, affected by surfactant molecules due to change of electrochemical capacity of these cells. The differences among of intensity on X-ray diffraction lines show that the preferred growth of the grains occurs in the presence of surfactant. Hence, the crystallographic orientation can be changed because the metal surface energy is modified by the surfactant absorption [28]. The variation on the crystallographic orientation in the presence of the surfactant can be attributed by having different crystal planes, with their various specific interactions. The low rate of the zinc discharge has been originated by the anionic SDBS surfactant, which has an inhibiting effect on the ZnO growth, showing less intensity. Furthermore, the increase of ZnO intensity diffraction line in the presence of cationic CTAB surfactant can be the other reason for high rate discharge reaction in these cells, causing more passivation.

3.6. Impedance parameters of the alkaline Zn/MnO_2 cell

3.6.1. Equivalent circuit modeling of Zn/MnO_2 cell

A useful and standard method for non-destructive investigation of electrochemical systems is electrochemical impedance spectroscopy (EIS) technique. EIS is generally used for the determination of the performance and the evaluation of kinetic parameters of battery electrodes and analysis of the kinetics of porous electrodes [29,30]. Cachet et al. [31] found that the fluorinated surfactant (F1110) remarkably reduce the rate of charge transfer in zinc deposition, on impedance data. Also, the presence of F1110 surfactant, in zincate electrolyte, prevents the growth of zinc dendrite. Then, it is interesting that we verify the inhibiting effect of surfactants in anodic portion by using the impedance technique. Since, the adsorption of organic inhibitors onto the zinc surface can increase the impedance of the undischarged cell.

In this paper, we took the EIS measurements on fresh primary alkaline AA-size Zn/MnO_2 cells at two different SOCs, viz., 0 and 100 and at 61 discrete frequencies in the range of 0.01–100,000 Hz using Solarton SI 1260B. The fitting of experimental data to the proposed theoretical models was done by means of Z-view software.

At SOC100, the Nyquist plots of CT and SD cells are represented in Fig. 9a and b, respectively. Also Fig. 10a and b shows the impedance spectra for these cells at SOC0. Moreover, the Nyquist plots of without surfactant cell are given in these figures.

In Fig. 9a, the transition and diffusion regions were conspicuous in CT cells at SOC100. The slope of diffusion line increased at low frequencies as follows: 0.05 CT < 0.1 CT < 0.01 CT cells (Fig. 9a). Hence, the slop of the imaginary verses real plot in 0.01 CT cell goes more to infinity, so the dc-impedance of the electrochemical 0.01 CT cell would be more infinite at low frequencies. Furthermore, the impedance of without surfactant cell shows capacitive loop plus transition and diffusion regions. It should be said that the straight line in low frequencies has been adjusted by using a transmission line between the numerous zinc particles which are involved in process of ZnO film formation.

Fig. 9b presents the Nyquist plots of without surfactant cell and SD cells, consequently, the slop of the transition and diffusion lines increased in this order: 0.1 SD < 0.05 SD < without surfactant < 0.01 SD cell. The Nyquist plots of 0.1 SD and 0.05 SD cells contain capacitive loops at SOC100 in the high frequencies. Therefore, such consideration shows that the electrochemical reactions take place not only under charge transfer control at the high frequencies but also occurred under diffusion control at the low frequencies. By contrast, in 0.01 SD cell, the shortest transition and diffusion line is appeared. It is to say, the ions transport may be occurred in short space on reaction sites close to the surface. It seems that the reaction-rate is controlled by anionic SDBS surfactant. Also, the charge transfer limitation increases at its high concentration, causing higher hindrance for the electrochemical reaction.

The low frequencies tail of the complex plane plots in charged cells at SOC100 (Fig. 9a and b) was converted into significant lower angles at SOC0 (Fig. 10a and b), this shape change is more apparent especially in SD cells. It is clear that in the low frequencies, at SOC100, the linear spike behavior is converted gradually into an additional semicircle one at SOC0 (Fig. 10a and b). The diffusion impedance bends more onto real axis at low frequencies. It becomes more similar to distorted semicircle at finite Warburg. This transition behavior is more observable in 0.05 SD and 0.1 SD cell, respectively. It could be said that decreasing of second semicircle diameter is resulted from stronger blocking effect and more preventing properties for electrochemical

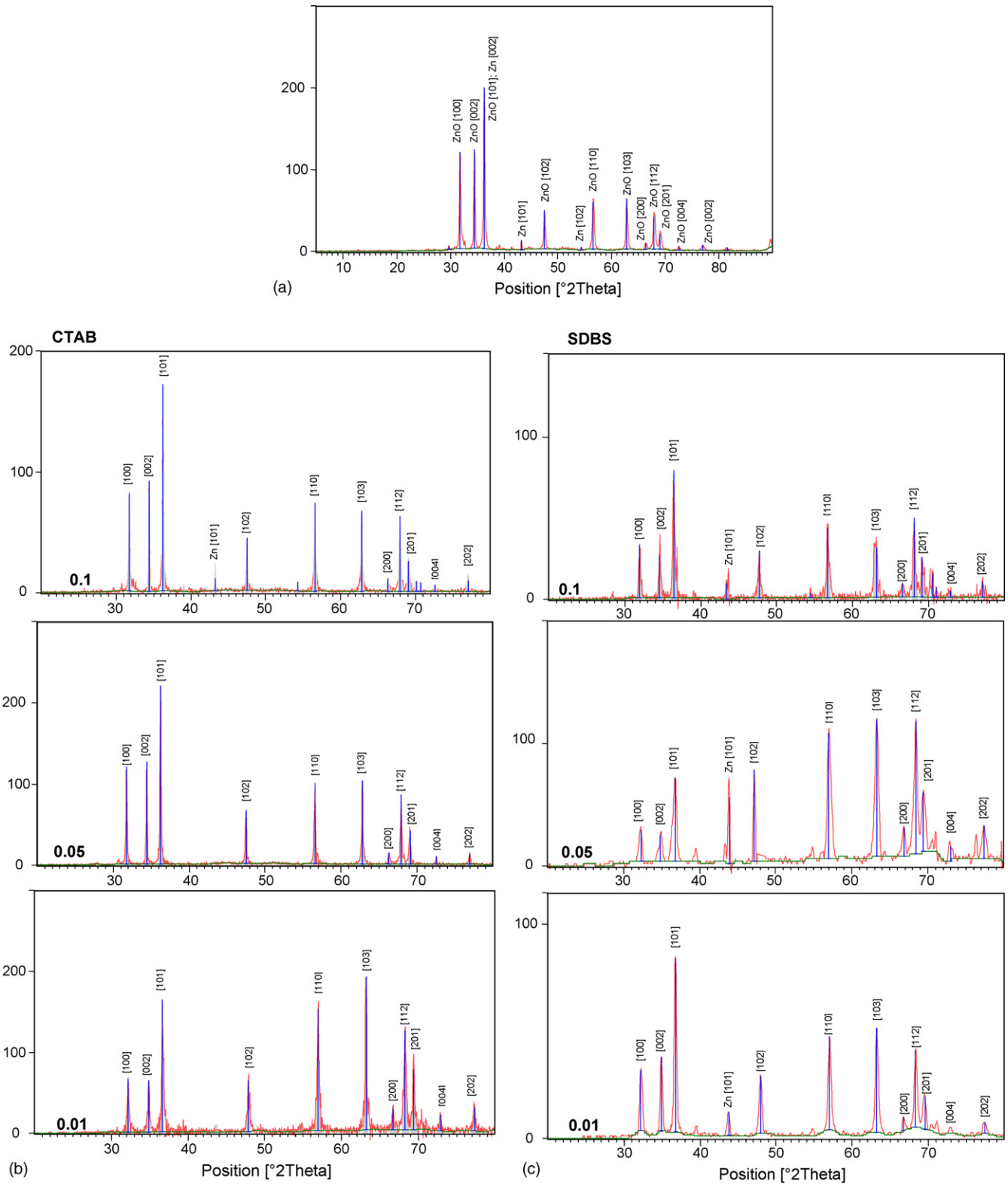

Fig. 8. Typical X-ray diffraction for discharged anode of the spent Zn–MnO_2 cells. (a) Without surfactant, (b) CT anode cells and (c) SD anode cells, with given amounts in Table 2.

reaction at its high concentration, causing less ZnO formation at SOC0.

The equivalent circuit is able to model the impedance values at SOC100 as shown in Fig. 11a. But at SOC0, we needed to modify the equivalent circuit, using RC section at high frequencies and a Z_{ZARC} impedance involving a constant phase element (CPE) at low frequencies (Fig. 11b) [32]. It should be said that the Warburg response has unit slope in a Nyquist plane. We can

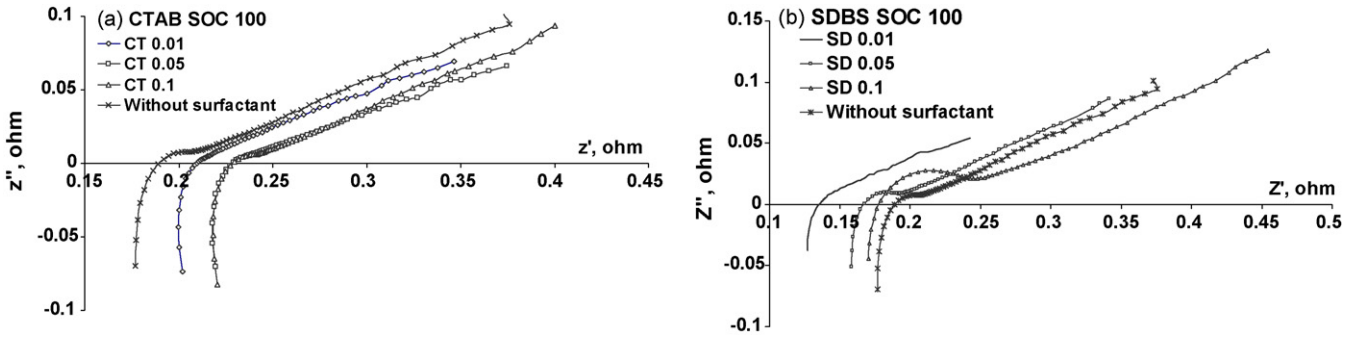

Fig. 9. Impedance diagrams at the SOC100. (a) Without surfactant and CT cells and (b) without surfactant and SD cells.

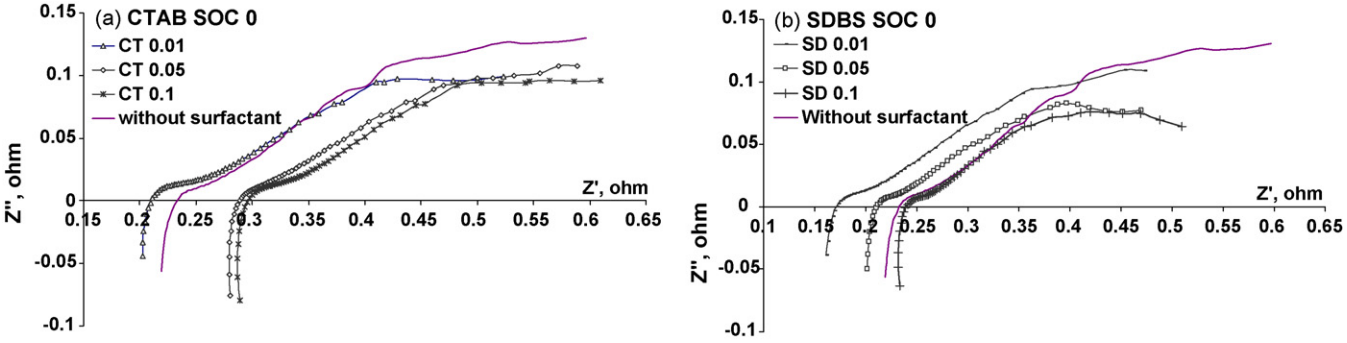

Fig. 10. Impedance diagrams at the SOC0. (a) Without surfactant and CT cells and (b) without surfactant and SD cells.

see that it is an especial case of CPE element whose impedance is in the form of $A_0(jw)^{-n}$, with "n" closed to 0.5, so we can use the CPE to describe such systems.

The ohmic resistance is represented by R_Ω and inductance behavior is shown at the high frequencies end by L. They are represented in two equivalent circuits. Good correlations were obtained with the proposed equivalent circuits during experimental EIS curves and fitting procedure happened. The extracted values of the two circuit elements were calculated from EIS curves, listed in Table 3.

3.6.2. *Variation of L, R_Ω, and C_{dl}*

Inductive components usually arise from the porous nature of the electrodes. The battery electrodes are usually porous and the porosity of the electrodes leads to impedance becoming inductive at high frequencies [33]. Therefore, L refers to inductors associated with the anode and the cathode that it was determined by data fitting for all cells, reported in Table 3. The data show that the Inductive values in the presence of cationic CTAB surfactant were higher than the others.

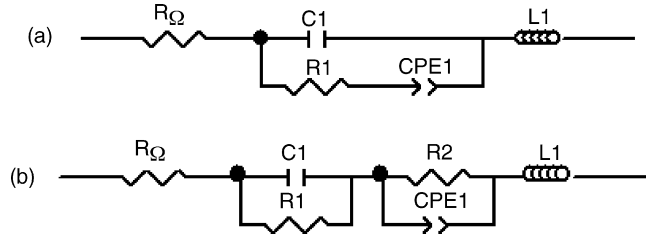

Fig. 11. Two circuits configurations are chosen to fit EIS data using Solarton SI 1260 over the frequencies band 0.01–10,000 Hz at discrete 61 frequencies.

The high frequencies intercept of the semicircle on the real axis is taken as ohmic resistance (R_Ω) of the cell, which includes the resistance of the electrolyte, separator and current collector, etc. [34]. Also, Yang and Lin [35] found that the impedance of Zn/MnO2 alkaline cells was affected by anodic composition because the impedance of the cell decreased when the electrolytic zinc powder was used in anodic gel.

In Table 3, R_Ω progressively rose with the increase of CTAB and SDBS surfactant concentration at both SOC (Table 3). In addition, the ohmic resistance in CT cells was higher than SD cells. As a result, R_Ω increases in the presence of cationic CTAB surfactant, while anionic SDBS surfactant declines ohmic resistance. Therefore, increasing of surfactant concentration causes higher ohmic resistance.

The double layer capacitance (C_{dl}), which related to the interface between the surface films and the active mass, can be closer to values of the capacity which related to adsorption phenomena. The value of the double layer capacitance depends on many variables including electrode potential, temperature, ionic concentration, types of ion, oxide layers, electrode roughness and impurity adsorption, etc. [36,37]. Helmoholtz in 1879 [38], Gouy in 1910 [39], Chapman in1913 [40] and Stern in 1924 [41] discovered that charges can be separated and form a double layer across a conductor and liquid electrolyte. The stored capacitance in the double layer is proportional to the surface area of the electrode and inversely proportional to the thickness of the double layer.

In Table 3, the comparison of the double layer capacitance for all cells at SOC100 shows that C_{dl} increased in the presence of cationic CTAB and it decreased when anionic SDBS surfactant was added to anodic gel. Also, the double layer capacitance of

Table 3
Values of the elements with two suggested circuits, 11a and 11b

Equivalent circuit 11a	SDBS SOC100			Without surfactant	CTAB SOC100		
Concentration ($g\,l^{-1}$)	*0.01*	*0.05*	*0.1*		*0.01*	*0.05*	*0.1*
L_1	6.40E−07	8.89E−07	1.01E−06	1.19E−06	1.20E−06	1.17E−06	1.32E−06
R_Ω	0.123	0.156	0.181	0.174	0.197	0.215	0.288
R_{ct}	0.0098	0.023	0.036	0.0216	0.009	0.0118	0.0111
C_{dl}	0.0024	0.0027	0.0029	0.0024	0.0041	0.0034	0.0028
CPE-P	0.311	0.271	0.257	0.28	0.281	0.262	0.263
CPE-T	18.74	10.45	7.22	9.28	13.27	12.43	6.28
Equivalent circuit 11b	SDB SSOC0			Without surfactant	CTAB SOC0		
Concentration ($g\,l^{-1}$)	*0.01*	*0.05*	*0.1*		*0.01*	*0.05*	*0.1*
L_1	6.69E−07	8.34E−07	1.02E−06	9.28E−07	7.30E−07	1.22E−06	1.24E−06
R_Ω	0.155	0.201	0.232	0.222	0.207	0.287	0.291
C_{dl}	0.008	0.007	0.01	0.006	0.0098	0.011	0.0094
R_{ct1}	0.0181	0.018	0.019	0.023	0.021	0.016	0.0236
R_{ct2}	1.035	0.514	0.513	0.93	1.42	0.807	0.798
CPE-P	0.345	0.399	0.432	0.407	0.331	0.378	0.375
CPE-T	6.228	6.461	6.356	5.5	5.98	5.43	5.69

0.01 CT and 0.05 CT cell was higher than the others. It is to say, C_{dl} of the undischarged cells increased by cationic CTAB surfactant absorption, affected by their concentration ranges, causing high surface area. Thus, cationic CTAB surfactant can increase discharge-rate, causing more activity on zinc surface and high dissolution-rate especially at low concentration.

In addition, with increasing surfactant concentration, less zinc utilization and less surface area resulted from inhibiting properties. Thus this behavior is mainly affected by kinds and amount of surfactant. As mentioned, higher surface area related to greater double layer capacitance at low concentration, so the zinc passivation occurs rapidly due to more activity on zinc surface.

3.6.3. Variation of R_{ct}

R_{ct} is determined by data fitting at SOC100 that is mainly related to the contact of impedances between zinc particles that was affected by surfactant. It was found that the charge transfer resistance and the Warburg coefficient of high surface area of MnO_2 cathode were very small and the corresponding double layer capacitance was very large. As a result, the impedance of the zinc anode was the essential constituent of the measured cell impedance [42].

Fig. 12a shows variation of charge transfer (R_{ct1}) for SD and CT cells at SOC100. It is obvious that the reduction of R_{ct} in CT cells is corresponded to easier charge transfer especially at the low surfactant concentration. It seems that electrical conductance of undischarged CT cells between the electrolyte solution and the metallic substrate improved in the presence of cationic CTAB surfactant. So such conductance causes higher surface area, more zinc dissolution, and flat discharge curve with higher capacity just in the first discharge step especially in 0.01 CT.

Moreover, increasing of R_{ct} is observed in this order: 0.01 SD < 0.05 SD < 0.1 SD cell (Fig. 12a). Thus, anionic SDBS surfactant can prevent dissolution reaction at undischarged SD cells through increasing charge transfer resistance, showing more inhibiting properties at high concentration.

We found that R_{ct} increases when anionic SDBS surfactant is added to anodic gel and it decreases in the presence of cationic CTAB surfactant cell, causing more activity on reaction sites for polarization, compared with free surfactant cell.

The resistance and capacitance of ZnO are reflected in the form of a semicircle in the low frequencies region of Nyquist plot at SOC0 [22], which were attributed to the size of the second semicircle. Fig. 12b shows the comparison of charge transfer resistance (R_{ct2}) in the discharged alkaline cells at SOC0. R_{ct2}

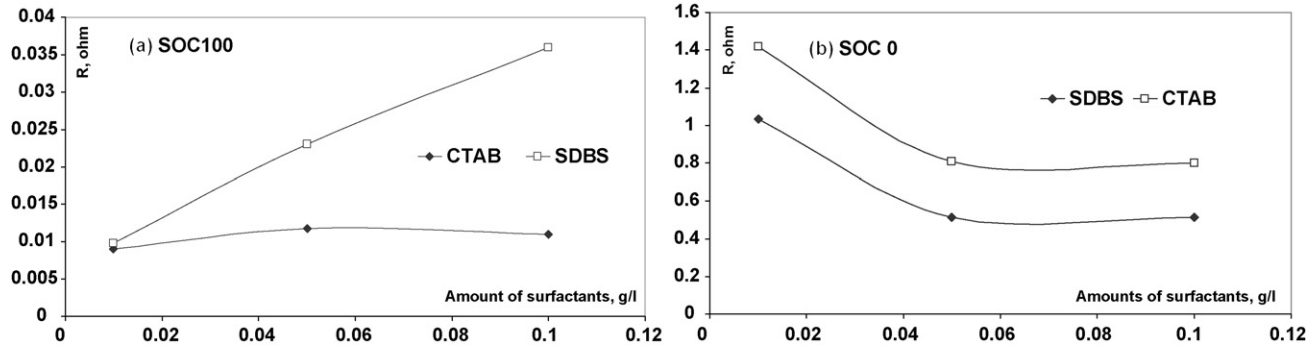

Fig. 12. Variations of charge transfer resistance. (a) R_{ct1} at SOC100 and (b) R_{ct2} at SOC0.

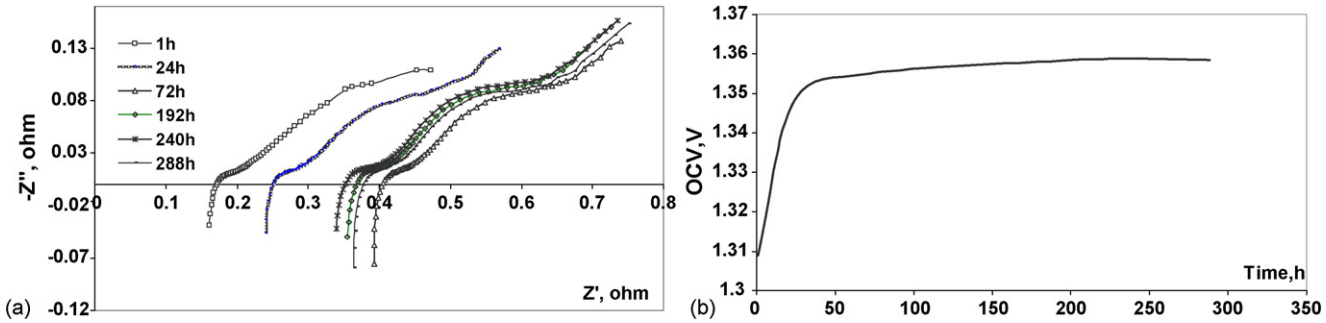

Fig. 13. Nyquist impedance plots of 0.01 SD cell during ageing time at SOC0. Corresponding ageing time is indicated (a). Variation of OCV in discharged 0.01 SD cell on ageing time (b).

increased in the presence of cationic CTAB while it decreased in SD cells. The high charge transfer resistance in discharged CT cells can be arisen from numerous zinc oxide particles or large inactive ZnO crystals formation. By contrast, in discharged SD cells, the decrease of the charge transfer resistance can take place through the formation of fine ZnO semiconductor on the zinc surface.

In addition, with increasing of surfactant concentration, R_{ct2} decreased. It can be related to less inactive zinc oxide formation during discharge process.

3.6.4. Nyquist plot at SOC0 on ageing time

On ageing time, we investigated the shape changes of Nyquist plots in the discharged 0.01 SD cell as shown in Fig. 13a. As mentioned, the Nyquist plot contains two semicircles at SOC0: The middle frequencies semicircle is due to charge transfer resistance in the presence of ZnO film (R_{ct}) and constant phase element (CPE), the low frequencies semicircle is due to diffusional impedance (Z_d). On ageing, the hump was gradually growing into a semicircle (as seen in Fig. 13a). The shape change of Nyquist plot mostly took place between 1 h and 7 days after that it was getting constant.

According to Fig. 13a, the charge transfer resistance in the discharged 0.01 SD cells, which was appeared by second semicircle diameter in the middle frequencies, decreases after 24 h rest step. It is to say, that the condition for subsequent discharge is provided on aging time. It seems that the condition for ions diffusion has improved on aging time. Therefore, the structure of ZnO layer plays an important role in the mass transport of ions and its activity. Also its OCV variation has been approximately constant after 24 h (Fig. 13b).

However, the high stored energy in SD cells can be logical reason for decreasing of second semicircle due to formation of ZnO passive film with active character and its capacity recovery.

3.7. Mechanism of zinc oxide formation in the anode gel

The reaction of ZnO formation was mentioned in Section 3.1. During discharge process, the conversion of zinc powder to zinc oxide proceeds via two steps: First, the zinc at the anode reacts with OH^- to form $Zn(OH)_4^{2-}$ i.e., the so-called "dissolution process" (reaction (3)). Then, zincate ions convert to zinc oxide i.e., the so-called "deposition process" or "precipitation process" (reaction (4)). The first step is an electrochemical reaction and thus involves electron transfer, such transfer of electrons takes place only on the conductive sites of the fresh zinc. The rate of the electrochemical reaction is therefore dependent on diffusion of ions and effective surface area of zinc.

The second step is a chemical reaction and proceeds at a rate which is zincate ions-dependent. The solubility of zincate ions determines the reaction-rate (4).

In discharge process, in the presence of anionic SDBS surfactant especially low concentration, the dissolution-rate of Zn^{2+} is slow from each zinc crystal, and therefore, the accompanying consumption of OH^- in the interior of the anode gel is likely to be counterbalanced by the diffusion of OH^-. Furthermore, the subsequent reaction of $Zn(OH)_4^{2-}$ to ZnO also occurs slowly because of low supersaturation of $Zn(OH)_4^{2-}$ in the vicinity of each parent zinc crystal. Since the rate of deposition (reaction (4)) is slow, newly formed ZnO tends to participate preferentially on the already deposited ZnO crystal, i.e., growth rate < nucleation rate. Thus, the fine zinc oxide layers develop on the anode surface in the presence of anionic SDBS surfactant. In the high concentration of surfactant, a regular crystal growth of ZnO with less needle morphology affects the penetration of electrolyte into micropores and ultimately decreases proton mobility in the zinc surface and restricts ions diffusion. This phenomenon affects on discharge performance of these cells, improving the total service life of SD cells, step by step.

Moreover, the formed passive film on the zinc electrode in SD cells has an active character, i.e., anionic SDBS surfactant decreases the dissolution-rate, especially when they consist of the semiconducting films of the fine ZnO crystal.

In discharge process, the formation of ZnO proceeds differently in the presence of cationic CTAB surfactant. The electrochemical reaction (i.e., reaction (3)) now proceeds so rapidly, zincate is mainly formed. As a result, the zinc tends to high solubility. Then, more zincate is generated especially in 0.01 CT cell. The zincate will therefore precipitate on any available surface, i.e., nucleation rate < growth rate. Thus, a non-uniform of zinc oxide is deposited on the surface through the high solubility of zincate in 0.01 CT cell. The results confirmed that the higher surface area and much easier electron transfer are provided in the presence of cationic CTAB surfactant

especially 0.01 CT cell. Therefore, it seems that the super saturation of zincate occurs in this order: CT 0.1 < CT 0.05 < CT 0.01. Therefore, increasing of cationic CTAB surfactant concentration hinders the zinc electrode shape change and ZnO non-homogenous deposition because of more inhibiting property. Also, the ZnO non-homogenous deposition affected on the development of inter-electrode short-circuit, causing premature capacity loss due to more passivation.

However, in CT cells, the passivation can proceed irreversibly through the formation of inactive coarse ZnO, having compact structure with high electrical resistance. Such a dense film completely blocks the anodic dissolution of zinc especially in 0.01 CT cell.

On the other hand, the enhancement of the zinc electrode performance depends mainly on solubility of formed zincate products during the anodic dissolution. Hence, the quality of zinc surface is depended on inhibiting performance.

4. Conclusion

The interest has been focused on the relationship between characteristic of surfactant additives in alkaline batteries and the chemistry involved in dissolution and passivation of zinc electrodes. It is to say that these processes are greatly influenced by the type and quantity of surfactant on the composition of the used electrolyte.

Surfactants are combined with an electrochemical zinc reaction. Then, anodic compartment containing surfactant and zinc metal operate as a substrate. When required potential for the zinc substrate reduction lies within the applied current (0.5 A), the zinc ions species will be deposited as organized morphology on the zinc surface by surfactant. As a result, the formation of certain templates with specified capacity induces individual electrochemical properties.

In the presence of cationic 0.01 g l^{-1} CTAB surfactant, the positively charged head groups of CTAB ($C_{19}H_{42}N^{+}$) cannot strongly organize Zn^{2+} species and form ZnO with larger size on the electrode surface. The smaller size and the well-shaped morphology of the particles at the high concentration is due to more adsorption of CTAB on the growing surface of ZnO, which affects crystal growth pattern and zinc passivation manner, causing inhibiting effect on zinc passivation. We found that the positively charged head groups of CTAB induce the more passivation on zinc surface, compared to without surfactant cell.

However, the formed ZnO film in the presence of anionic SDBS surfactant shows dramatic changes in shapes of crystals. The results indicate that the negative charged head groups of SDBS ($C_{19}H_{31}SO^{-}{}_{3}$) cooperation interacts the Zn surface to form in situ templates on the electrode. These templates decrease the zinc electrode passivation and increase charge transfer resistance on zinc electrode before discharging especially at high concentration. Thus, higher total service life was gradually obtained (step by step) in the corresponded cells, which revealed smaller grain size with less ZnO intensity on diffraction line.

Acknowledgement

The authors would like to thank Mrs. Karimi for helpful discussion.

References

[1] J. McBreen, J. Electroanal. Chem. 168 (1984) 415.
[2] D.T. Chin, R. Sethi, J. McBreen, J. Electrochem. Soc. 129 (1982) 2677.
[3] C. Juhel, B. Beden, C. Lamy, J.M. Leger, Electrochim. Acta 35 (1991) 678.
[4] K. Bass, P.J. Mitchell, G.D. Wilcox, J. Smith, J. Power Sources 39 (1992) 273.
[5] N.C. Cahoon, H.W. Holland, in: G.W. Heise, N.C. Cahoon (Eds.), The Primary Batteries, vol. 1, J. Wiley & Son, New York, 1971, p. 239.
[6] S.A.G.R. Karunathilaka, N.A. Hampson, J. Appl. Electrochem. 10 (1980) 357.
[7] J.Y. Huot, M. Malservisi, J. Power Sources 96 (2001) 133–139.
[8] O. Kardos, Plating 61 (1974) (2) 29, (3) 129, (4) 316.
[9] V.K. Nartey, L. Binder, K. Kordesch, J. Power Sources 52 (1994) 217.
[10] R. Shivkumar, G.P. Kalaigan, T. Vasudevan, J. Power Sources 75 (1998) 90.
[11] J.L. Zhu, Y.H. Zhou, C.Q. Gao, J. Power Sources 72 (1998) 231.
[12] C. Cachet, B. Saidani, R. Wiart, J. Electrochem. Soc. 138 (1991) 678.
[13] H. Yang, Y. Cao, X. Ai, L. Xiao, J. Power Sources 128 (2004) 47–101.
[14] Milton J. Rosen, Surfactant and Interfacial Phenomena Book, 2nd ed., John Wiley of New York, 1989, p. 39.
[15] U. Retter, M. Tchachnikova, J. Electroanal. Chem. 550/551 (2003) 201.
[16] J.F. Rusling, Coll. Surf. 123/124 (1997) 81.
[17] J.O. Besenhard, J. Gurtler, P. Komenda, A. Paxions, J. Power Sources 20 (1987) 257.
[18] J. Liu, et al., Mater. Lett. 59 (2005) 3710.
[19] K. Matsuki, M. Sugawara, A. Kozawa, Prog. Batteries Battery Mater. 11 (1992) 25.
[20] A.L. Rudd, C.B. Breslin, Electrochim. Acta 45 (2000) 1571.
[21] L. Binder, W. Odar, K. Kordesh, J. Power Sources 6 (1981) 271.
[22] S. Rodrigues, N. Munichandraiah, A.K. Shukla, J. Appl. Electrochem. 30 (2000) 371.
[23] M. Yano, S. Fujitani, K. Nishio, Y. Akai, M. Kurimura, J. Power Sources 74 (1998) 129.
[24] T.S. Lee, J. Electrochem. Soc. 118 (1971) 1278.
[25] T.P. Dirkse, J. Electrochem. Soc. 101 (1954) 328.
[26] R. Shivkumar, G. Paruthimal Kalaignan, T. Vasudevan, J. Power Sources 55 (1995) 53.
[27] D.Y. Li, J.A. Szpunar, Electrochim. Acta 42 (1997) 47.
[28] E. Buderski, G. Staikov, W.J. Lorenz, Electrochemi (a) Phase Formation and Growth, VCH, Weinhiem, 1996.
[29] F. Huet, J. Power Sources 70 (1998) 59.
[30] M.J. Root, J. Appl. Electrochem. 25 (1995) 1057.
[31] C. Cachet, Z. Chemi, R. Wiart, Electrochim. Acta 32 (1987) 465.
[32] S.R. Nelatury, P. Singh, J. Power Sources 132 (2004) 309.
[33] N.A. Hampson, S.A.G.R. Karunathilaka, P. Leek, J. Appl. Electrochem. 10 (1980) 7.
[34] D. Qu, J. Power Sources 102 (2001) 270.
[35] C.C. Yang, S.J. Lin, J. Power Sources 112 (2002) 174.
[36] E. Barsoukov, J.R. Macdonald (Eds.), Impedance Spectroscopy; Theory, Experiment, and Applications, 2nd ed., Wiley Interscience Publications, 2005.
[37] A.J. Bard, L.R. Faulkner, Electrochemical Methods; Fundamentals and Applications, Wiley Interscience Publications, 2000.
[38] H. Helmoholtz, Annalen der Physic und Chemie, Bd. VII, H.7 (1879) 337.
[39] G. Gouy, J. Phys. 9 (1910) 457.
[40] D.L. Chapman, Philos. Mag. 25 (1913) 475.
[41] O. Stern, Z. Elektochem. 30 (1924) 508.
[42] S. Rodrigues, N. Munichandraiah, J. Power Sources 87 (2000) 12.